5-1-2007

Global profiles of compressional ultralow frequency wave power at geosynchronous orbit and their response to the solar wind

Jeff Sanny
Loyola Marymount University, jeff.sanny@lmu.edu

D. Judnick
Loyola Marymount University

M. B. Moldwin
University of California, Los Angeles

David Berube
Loyola Marymount University, david.berube@lmu.edu

D. G. Sibeck
NASA Goddard Space Flight Center

Global profiles of compressional ultralow frequency wave power at geosynchronous orbit and their response to the solar wind

J. Sanny,[1] D. Judnick,[1] M. B. Moldwin,[2] D. Berube,[2] and D. G. Sibeck[3]

Received 28 August 2006; revised 16 February 2007; accepted 23 February 2007; published 26 May 2007.

[1] We investigate the global local-time profiles of compressional wave power in three ultralow frequency (ULF) bands corresponding to Pc3, Pc4, and Pc5 pulsations using magnetic field data from the geosynchronous GOES satellites. The global power profiles of the three frequency bands are studied for low, moderate, and high levels of geomagnetic activity based on the *Dst* index. We also consider the seasonal variation of the ULF power profiles, as well as the effects of solar wind and interplanetary magnetic field (IMF) parameters. For high geomagnetic activity, we find that the greatest power is associated with compressional Pc5 pulsations in the afternoon sector; for low geomagnetic activity, ULF power levels are consistently highest in the tail region. A summer power minimum in all three frequency bands is observed in our study of seasonal variation, while higher power levels occur around local midnight throughout the year. The enhancement of ULF power by high solar wind velocity and pressure is greater for the lower-frequency waves. Furthermore, solar wind plasma parameters have a significantly greater influence on ULF wave power than IMF parameters like cone angle and northward/southward orientation.

Citation: Sanny, J., D. Judnick, M. B. Moldwin, D. Berube, and D. G. Sibeck (2007), Global profiles of compressional ultralow frequency wave power at geosynchronous orbit and their response to the solar wind, *J. Geophys. Res.*, *112*, A05224, doi:10.1029/2006JA012046.

1. Introduction

[2] Since their discovery in the mid-nineteenth century, ultralow frequency (ULF) waves have been the subject of numerous investigations whose results have provided a significant contribution to our understanding of the dynamics of Earth's magnetosphere. ULF pulsations are classified as either continuous, with a quasi-sinusoidal signature, or irregular, with a noise-like signature. The five subclasses of continuous pulsations are distinguished by period as Pc1 (0.2–5 s), Pc2 (5–10 s), Pc3 (10–45 s), Pc4 (45–150 s), and Pc5 (150–600 s), while the two subclasses of irregular pulsations are Pi1 (1–40 s) and Pi2 (40–150 s) [*Jacobs et al.*, 1964].

[3] Many surveys of the occurrence rate and properties of ULF pulsations have been based on measurements at ground stations, which allow for continuous coverage over large segments of Earth's surface. Some examples include the works of *Saito et al.* [1989], who studied the seasonal dependence of Pc3–Pc5 wave power using auroral zone stations, *Dyrud et al.* [1997], who investigated the latitudinal and local distributions of Pc1 and Pc2 events using stations in Arctic Canada and Antarctica, and *Howard and Menk* [2005], who used the International Monitor for Auroral Geomagnetic Effects (IMAGE) magnetometer array to study dayside Pc3 and Pc4 waves.

[4] Statistical in situ surveys of ULF waves have used spacecraft with both geosynchronous and elliptical orbits. For example, *Kokubun et al.* [1989] used magnetic field and particle flux observations from the geosynchronous ATS 6 to examine the dawn-dusk asymmetry of Pc4 and Pc5 wave characteristics and their associated proton flux modulations; *Anderson et al.* [1990] developed a comprehensive database of Pc3–Pc5 activity observed from $L = 5$ to $L = 9$ by the AMPTE/CCE satellite. Other similar surveys of note include those by *Zhu and Kivelson* [1991], who used magnetic field and plasma data from the ISEE 1 and 2 spacecraft to investigate compressional ULF waves in the outer magnetosphere, *Takahashi and Anderson* [1992], who examined the spatial distribution of ULF energy in the inner magnetosphere from AMPTE/CCE magnetic field data, and *Lessard et al.* [1999], who used dynamic spectra of magnetic field data from the AMPTE/IRM spacecraft to determine occurrence rates of different types of pulsations over all local times (LTs) from $L = 6$ to $L = 20$.

[5] Although ULF pulsations may be generated by various mechanisms (for a listing, see [*Anderson*, 1994]), their energy must ultimately originate from the solar wind. Recent studies on the correlation between solar wind properties and ULF waves have determined that variations in the upstream solar wind number density and dynamic pressure precede compressional magnetic field variations at geosynchronous orbit [*Kepko et al.*, 2002; *Kepko and*

[1]Physics Department, Loyola Marymount University, Los Angeles, California, USA.
[2]Institute of Geophysics and Planetary Physics, University of California, Los Angeles, California, USA.
[3]NASA Goddard Space Flight Center, Greenbelt, Maryland, USA.

0148-0227/07/2006JA012046

Spence, 2003]. Numerous investigations have also shown the occurrence and power of ULF pulsations to be strongly dependent on the velocity of the solar wind [e.g., see *Junginger and Baumjohann*, 1988; *Engebretson et al.*, 1998]. Finally, *Chi et al.* [1994] found that intense Pc3 and Pc4 signals were observed when the cone angle of the interplanetary magnetic field (IMF) was less than 45° and ceased when the cone angle increased to larger values.

[6] In this paper, we investigate the global local-time profiles of ULF wave power in the Pc3, Pc4, and Pc5 frequency bands. Contributions to the power may be due to continuous as well as irregular pulsations. High time resolution magnetic field strength data from the geosynchronous GOES satellites are used in the analysis. We collected all available files from the 1984–1988 data set of GOES magnetic field measurements and filtered them with the three Pc frequency passbands. The average hourly wave power for each passband was then determined using Fourier analysis.

[7] Most surveys of ULF pulsations have been based on the approach in which the events are first identified, their properties tabulated, and a statistical analysis presented. In this regard, our methodology is somewhat unconventional and is most comparable to that of *Takahashi and Anderson* [1992], who studied the distribution of ULF energy ($f <$ 80 mHz) in the inner magnetosphere ($L = 2.5–6.5$). Using a magnetic field database exceeding 4 years, the authors investigated the *Kp* dependence of the spatial distribution of ULF energy. With a similarly large collection of geosynchronous magnetic field data, we extend their work to investigate how the global power profile of ULF energy depends on geomagnetic activity, season, solar wind, and IMF properties.

[8] We begin by studying the global wave power profiles of the three ULF frequency bands for low, moderate, and high levels of geomagnetic activity based on the *Dst* index. We then consider the seasonal variation of these profiles. Finally, we investigate how the ULF power profiles respond to solar wind velocity, dynamic pressure and pressure variability, IMF cone angle, and B_z. Some of the questions considered include the following: What are the differences in the geosynchronous responses of power within the three frequency bands to increasing geomagnetic activity? Does ULF wave power exhibit the minimum in geomagnetic activity at the solstices that is commonly attributed to reduced coupling to the solar wind? What are the relative global responses of the three frequency bands to increased solar wind velocity, and to increased variability in the solar wind dynamic pressure? Previous studies using ground stations have indicated that Pc3 activity is biased toward intervals of small IMF cone angle [e.g., see *Chi et al.*, 1994]. Is this effect exhibited clearly at geosynchronous orbit, and in which sector is this bias greatest? Furthermore, is there any corresponding enhancement in Pc4 and Pc5 activity? There has been some disagreement on whether there is any correlation between ULF power levels and IMF B_z. Is this correlation apparent at any local time for any of the three ULF bands?

[9] This work is an extension of the study by *Sanny et al.* [2002], in which the variability of the dayside geosynchronous magnetic field strength was examined during intervals of reduced geomagnetic activity. With its extensive database, our present study is one of the most comprehensive investigations of ULF power and its response to geomagnetic conditions, the solar wind, and the IMF. While the results are clearly qualitative, we hope that they may be of use as a reference to other, more in-depth works. We present an example of such a project at the end of this paper.

2. Data Sets

[10] All geosynchronous magnetic field measurements used were made by the GOES 5 and GOES 7 satellites [*Grubb*, 1975]. Twenty-four-hour data files from GOES 5 and GOES 7, with a time resolution of 3 s, make up a collection available from day 229, 1984 to day 366, 1988 from http://sd-www.jhuapl.edu, the Web site of the Johns Hopkins University Applied Physics Laboratory. In order to cover the entire interval, we used observations by GOES 5 from day 229, 1984 to day 84, 1987, and by GOES 7 from day 85, 1987 to day 366, 1988. Throughout the entire period, the LT positions of the two spacecraft were related to universal time (UT) by approximately LT = UT − 5 h.

[11] Available 24-h data files from the 1984–1988 data set of GOES magnetic field strength measurements were despiked and filtered into the different ULF frequency passbands, and the average hourly wave power for each passband was found by applying a fast Fourier transform (FFT) to each hourly window (1200 points). The sampling rate allowed us to determine powers only for the Pc3, Pc4, and Pc5 bands. Hours during which the GOES spacecraft made magnetopause crossings were removed from our database. We also visually inspected all the hourly intervals containing high wave power values to ensure that the power was not due to unwanted artifacts, such as "steps," in the data that were not removed by our despiking program. Any hour found to contain such artifacts was removed from the database. Finally, we defined (and eliminated) "broadband noise" as data intervals in which the ULF powers of the three passbands all exist between a factor of 10 of each other.

[12] Hourly values of the *Dst* index were obtained from the Web site of the World Data Center for Geomagnetism in Kyoto (http://swdcdb.kugi.kyoto-u.ac.jp). Hourly averages of solar wind and IMF parameters were downloaded from the OMNIWeb site of the National Space Science Data Center (http://nssdc.gsfc.nasa.gov/omniweb).

3. Statistical Survey

3.1. ULF Power Profile Versus the *Dst* Index

[13] We begin by investigating the local-time ULF power profile for different ranges in the values of the *Dst* index. The three ranges considered are $Dst < -80$ nT (intervals with high levels of geomagnetic activity), -80 nT $\leq Dst <$ -20 nT (intervals with moderate geomagnetic activity), and -20 nT $\leq Dst \leq +20$ nT (intervals with low geomagnetic activity). Figure 1 shows the local-time distribution of the hourly averages of the logarithm of the power spectral density (psd) of ULF waves in the three frequency bands. The panels, from top to bottom, display the power profiles in the Pc5, Pc4, and Pc3 bands, respectively. We depict the uncertainty in the average hourly wave power within each bin in this and all subsequent figures by the standard

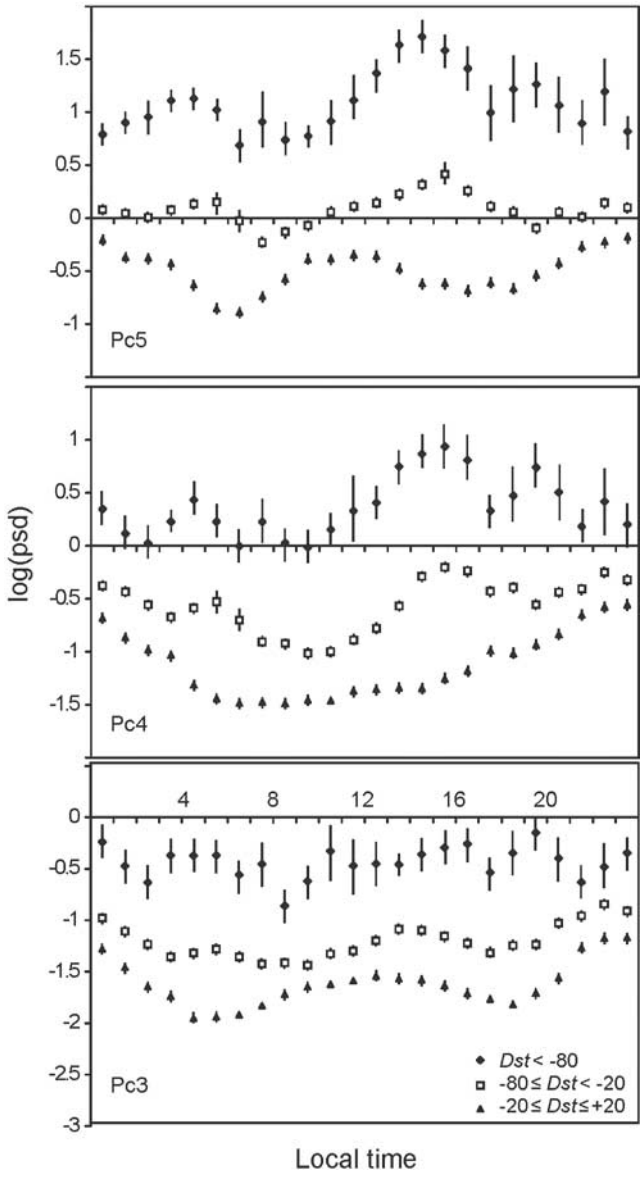

Figure 1. Global profiles of ULF wave power for low, moderate, and high levels of geomagnetic activity.

deviation from the mean $\pm\sigma_m = \pm\sigma/\sqrt{N}$, where N is the number of data points in the bin and σ is the standard deviation of their values. The average values of N for the ranges $Dst < -80$ nT, -80 nT $\leq Dst < -20$ nT, and -20 nT $\leq Dst \leq +20$ nT are around 20, 400, and 800, respectively. The labels "Pc5," "Pc4," and "Pc3" in all figures refer to the corresponding frequency bands and not to the type of pulsation.

[14] With the increase in geomagnetic activity, a prominent peak in the ULF power in the Pc5 band is formed in the afternoon sector. This peak is most likely associated with compressional Pc5 waves, which primarily occur in the afternoon and dusk at geosynchronous orbit (a number of references are listed in the review by *Anderson* [1994]). Compressional Pc5 waves have been found to be well correlated to substorm activity [*Barfield and McPherron*, 1978], and this is manifested in the peak in the first panel of Figure 1. A secondary Pc5 peak is formed near dawn. Previous surveys have also found a peak in Pc5 power in the morning sector [e.g., *Kokubun*, 1985; *Baker et al.*, 2003]. Surveys of Pc4 pulsations have indicated that they occur predominantly in the afternoon at geosynchronous orbit [*Arthur and McPherron*, 1981; *Takahashi and McPherron*, 1984]. This is manifested in the afternoon peak in wave power for the Pc4 band that is formed as geomagnetic activity increases. Unlike the other bands, there does not appear to be any local-time dependence Pc3 wave power for high levels of geomagnetic activity.

[15] During periods of low geomagnetic activity, we observe a prenoon peak in the power of the Pc5 band. This peak may be associated with pressure pulses. With the typical spiral IMF orientation, the prenoon magnetopause lies behind the quasi-parallel bow shock, so this is the region where foreshock/bow shock pressure pulses would strike and launch fast mode waves. A broad, low peak in the Pc3 band power appears throughout the dayside during quiet times, possibly a manifestation of upstream energy. In addition, the wave power is at elevated levels in the tail region for all three bands, perhaps because of the occurrence of ULF waves during the quiet periods following high geomagnetic activity.

3.2. Seasonal Dependence of the Global ULF Power Profile

[16] It has been known for well over a century that geomagnetic activity is more intense at the equinoxes than at the solstices. This effect is commonly attributed to the changing orientation of Earth's dipole, which modifies the shape of the magnetosphere and its coupling to the solar wind [*Russell and McPherron*, 1973]. As a result, solar wind input is strongest at the equinoxes. An alternate view was provided by *Cliver et al.* [2000], who suggested that this effect is not due to enhanced coupling at the equinoxes but rather a loss of coupling efficiency at the solstices. The authors also noted that the *am* and the *Dst* indices exhibited the characteristic seasonal variation.

[17] With our database of over 4 years, we are able to examine both the seasonal and the diurnal variations of activity. However, we do so from the perspective of ULF wave power. Our results are displayed in Figure 2. In order, the top-to-bottom panels show the seasonal variation versus the diurnal variation in the wave power of the Pc5, Pc4, and Pc3 frequency bands. In all three panels, the summer minimum in the power is clearly exhibited. There is a strong local minimum in the Pc4 band power around noon, while the minima of the Pc5 and Pc3 bands appear to be widely distributed on the dayside. Elevated power levels are observed around local midnight for all three frequency bands and are likely due to Pi1 and Pi2 activity associated with substorms [*Sigsbee et al.*, 2002]. While no seasonal variation in this nightside power can be discerned from Figure 2, a statistical study by *Borovsky and Nemzek* [1994] does indicate that there is a lower substorm occurrence rate during the summer. Near the equinoxes, the power maxima for all three pulsation bands are located in the afternoon sector.

[18] The seasonal variation in ULF wave power correlates well with the occurrence of magnetic storms, generally more intense and numerous at the equinoxes than at the solstices. During the interval of our database (September

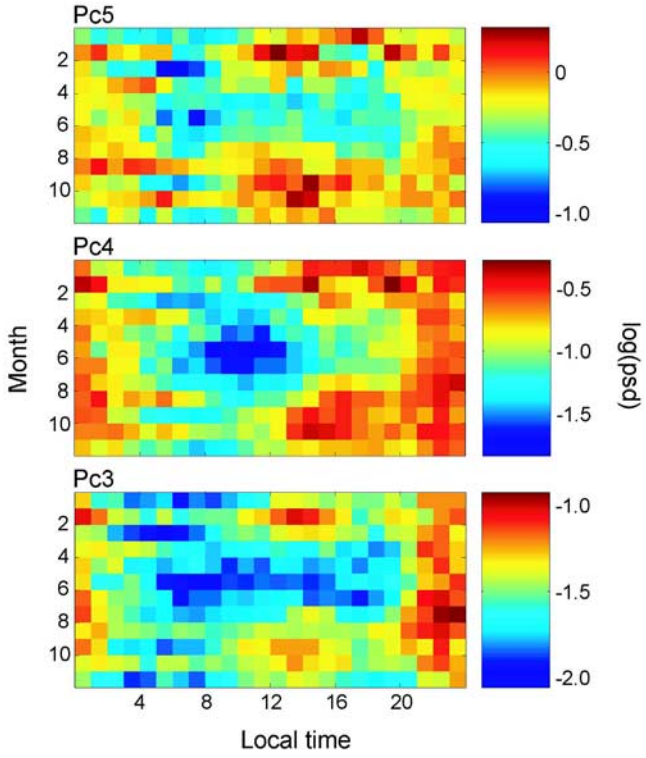

Figure 2. Seasonal variation versus diurnal variation in ULF wave power.

1984 to December 1988), we found 18 storms with a minimum $Dst \leq -100$ nT. Only two of these major storms occurred during the months of May, June, and July, which coincide with the summer minimum in geomagnetic activity.

3.3. Global Power Profile Versus Solar Wind and IMF Properties

3.3.1. Solar Wind Velocity

[19] The occurrence and intensity of ULF waves have been shown to be well correlated with solar wind velocity. For example, *Engebretson et al.* [1998] found that the Pc5 wave power observed at two ground stations, in the auroral zone and near the cusp region, both exhibited power law dependences on the solar wind velocity. *Junginger and Baumjohann* [1988] also noted significant correlations between the Pc5 power and the solar wind velocity from measurements made at geosynchronous orbit. A similar correspondence between solar wind velocity and Pc3 and Pc4 pulsations has also been observed [*Greenstadt et al.*, 1979a; *Yumoto et al.*, 1987]. Such results support the premise that the Kelvin-Helmholtz instability [*Southwood*, 1979] is a primary cause of toroidal magnetospheric pulsations. This effect produces surface wave-like disturbances at the magnetospheric boundary leading to the generation of Alfvén waves inside the magnetosphere [*Junginger and Baumjohann*, 1988].

[20] In our survey, we compared geosynchronous ULF power for "high" and "low" ranges of solar wind velocities: $V > 450$ km/s and $V < 400$ km/s. Our results are shown in Figure 3. All three frequency bands exhibit strong enhancements in wave power over the entire dayside during intervals of elevated solar wind velocities. This effect is much less pronounced on the nightside. The greatest changes in the Pc4 and Pc5 band powers occur in the late afternoon where the power increased by about a factor of 15. The greatest change in the Pc3 band power appears to peak just slightly after local noon and corresponds to a smaller increase of about a factor of 8. The weaker dependence of Pc3 pulsations on solar wind velocity has been noted in other studies [e.g., *Greenstadt et al.*, 1979b; *Odera*, 1986].

3.3.2. Solar Wind Dynamic Pressure and Variability of the Dynamic Pressure

[21] ULF pulsations in the magnetosphere have been postulated to be directly driven by variations in the solar wind dynamic pressure. *Kepko et al.* [2002] presented two ULF events in which the time series and spectral properties of the solar wind dynamic pressure far upstream from Earth match those of the geosynchronous magnetic field measure-

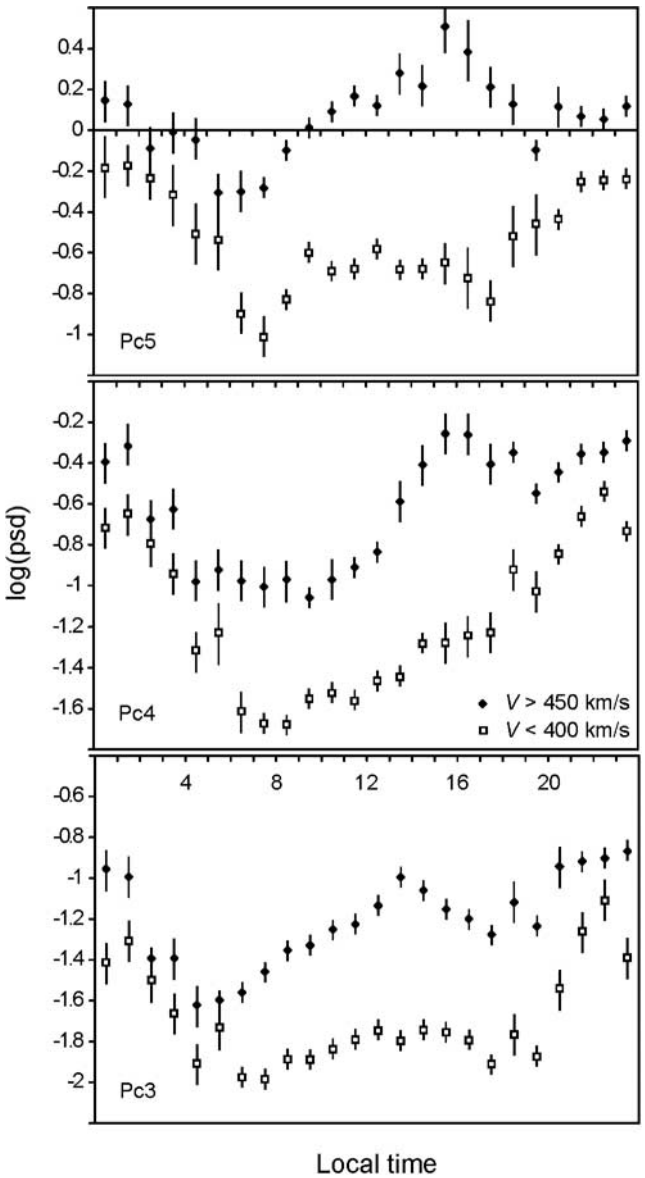

Figure 3. Global profiles of ULF wave power for solar wind velocity in the ranges $V > 450$ km/s and $V < 400$ km/s.

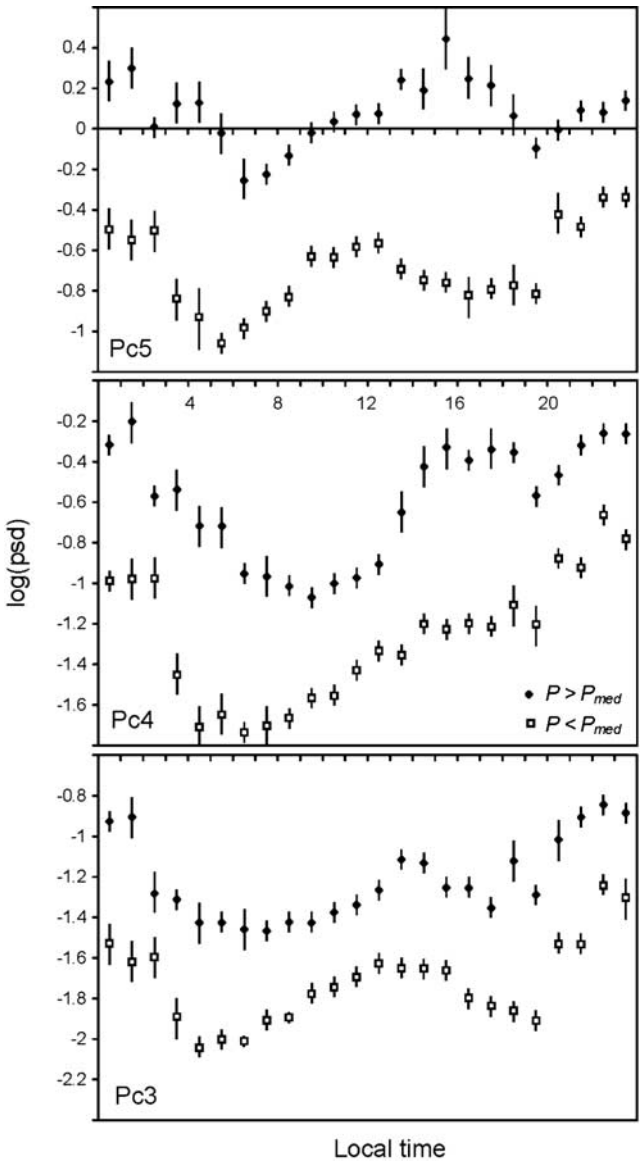

Figure 4. Global profiles of ULF wave power for solar wind dynamic pressure above and below its median value.

ments. Similar results were obtained by *Kepko and Spence* [2003] based on their analysis of six events. The authors suggested that periodic solar wind dynamic pressure oscillations alter the size of the magnetospheric cavity, resulting in corresponding oscillations of the magnetospheric field. The best correlations between upstream and magnetospheric variations occurred for frequencies in the Pc5 range, while the spectral content differed significantly for higher frequencies. At these higher frequencies, the solar wind density structures may lose coherence between the times when they are observed by the monitoring spacecraft to the times when they strike the magnetosphere.

[22] We examined the global power profiles of the three ULF bands in terms of solar wind dynamic pressure as well as the variability of the dynamic pressure. Figure 4 is a comparison of power profiles above and below the median value of the dynamic pressure (~2.5 nPa). There is a strong similarity in the power profiles for *Dst*, *V*, and *P* as indicated in Figures 1, 3, and 4. It is likely that *Dst* activity was driven by recurrent interactions with high-speed streams in the solar wind, in which case high or low *Dst* activity would correspond to high or low values of *V* and *P*, respectively.

[23] A measure of the variability of the solar wind dynamic pressure P_{var} can be determined from available solar wind data using the error propagation equation [*Bevington and Robinson*, 1992]:

$$\sigma_x^2 \approx \sigma_u^2\left(\frac{\partial x}{\partial u}\right)^2 + \sigma_v^2\left(\frac{\partial x}{\partial v}\right)^2 + 2\sigma_{uv}^2\left(\frac{\partial x}{\partial u}\right)\left(\frac{\partial x}{\partial v}\right),$$

where σ_x, σ_u, and σ_v are the standard deviations of the quantities x, u, and v, respectively, and σ_{uv}^2 is the covariance between u and v. Applying this equation to the solar wind dynamic pressure $P = mNV^2$, we obtain for the variability of P:

$$P_{\mathrm{var}} = mV\sqrt{V^2N_{\mathrm{var}}^2 + 4N^2V_{\mathrm{var}}^2 + 4NV\sigma_{NV}^2},$$

where m is the proton mass, N is the proton number density, V is the flow speed, N_{var} and V_{var} are the standard deviations of N and V, respectively, and σ_{NV}^2 is the covariance between N and V.

[24] A comparison of the global wave power profile for our calculated values of P_{var} above and below its median value (~0.30 nPa) is shown in Figure 5. Except for minor differences, the enhancements observed in the wave power for high values of solar wind dynamic pressure and pressure variability are similar. This is not unexpected, as the variability of the solar wind dynamic pressure has been shown to increase with the magnitude of the dynamic pressure [*Sanny et al.*, 2002].

[25] The ULF wave power in all three frequency bands are enhanced globally by increased variability in the solar wind dynamic pressure. Consistent with the results of *Kepko et al.* [2002], the power enhancements appear to be frequency-dependent, with the highest frequency waves exhibiting the smallest increase and the lowest frequency waves exhibiting the largest increase in power.

3.3.3. IMF Cone Angle

[26] Solar wind control of Pc3 and Pc4 activity was investigated by *Chi et al.* [1994], who noted that strong ULF wave activity was observed across the Institute of Geological Sciences ground magnetometer array for a period of about 12 hours when the interplanetary magnetic field (IMF) cone angle θ was less than 45°. When the cone angle increased to large values, the Pc3 and Pc4 signals ceased. Furthermore, peak frequencies in the Pc3 band were approximately the same as the frequency of upstream waves observed by ISEE 1 and 2. This observed correlation between the frequency in the Pc3 band and the frequency of upstream waves provides strong evidence that Pc3 waves have a source in the foreshock region. Waves generated there by backstreaming ions convect back through the shock and against the magnetopause. Since no such similarity in frequency was found for the Pc4 waves, the authors concluded that these waves were generated by a different mechanism. Similar findings were made by *Chi et al.* [1998], who studied dayside statistical relationships between solar wind parameters and magnetometer data from

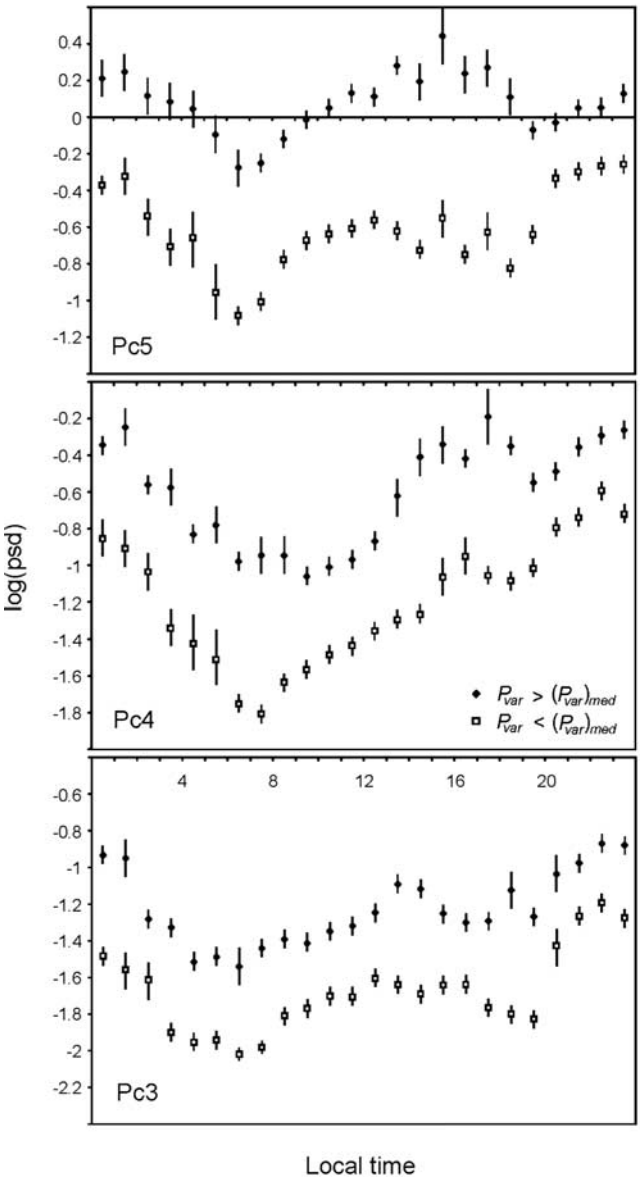

Figure 5. Global profiles of ULF wave power for solar wind dynamic pressure variability above and below its median value.

the Mount Clemens station (MCL, $L = 3$) of the Air Force Geophysics Laboratory (AFGL) Magnetometer Network.

[27] We considered the local-time distributions of ULF power for $\theta \geq 60°$ and for $\theta \leq 45°$, as shown in Figure 6. For pulsations in the Pc5 and Pc4 bands, there did not appear to be any extended region over which there was a significant difference in wave power between large and small cone angles. The only observed dependence of wave power on cone angle over an extended region occurred for the Pc3 band. On the dayside from about 9 LT to 13 LT, ULF power in this band was enhanced by about a factor of 3 for small values of the cone angle. Our results are in general agreement with *Chi et al.* [1994, 1998] and provide further evidence that the upstream foreshock is the energy source of Pc3 pulsations.

3.3.4. IMF B_z

[28] *Chi et al.* [1998] also noted that Pc5 power observed at the Mount Clemens station was particularly enhanced for periods of southward IMF. They suggested two possible sources for this activity. The first is substorm-related, with energy released by reconnection in the magnetotail and the generation of compressional Pc5 waves by the westward-moving ion injection. The second energy source may be flux transfer events that occur as a result of magnetic reconnection on the dayside magnetopause during southward IMF. In contrast, *Junginger and Baumjohann* [1988] found that the power and occurrence of Pc5 pulsations observed at geosynchronous orbit did not depend significantly on any of the IMF components. In fact, a greater number of events occurred when IMF $B_z > 0$ than when $B_z < 0$. Hence the authors ruled out flux transfer events as a dominant mechanism for the conversion of solar wind kinetic energy into pulsation energy. Similarly, a

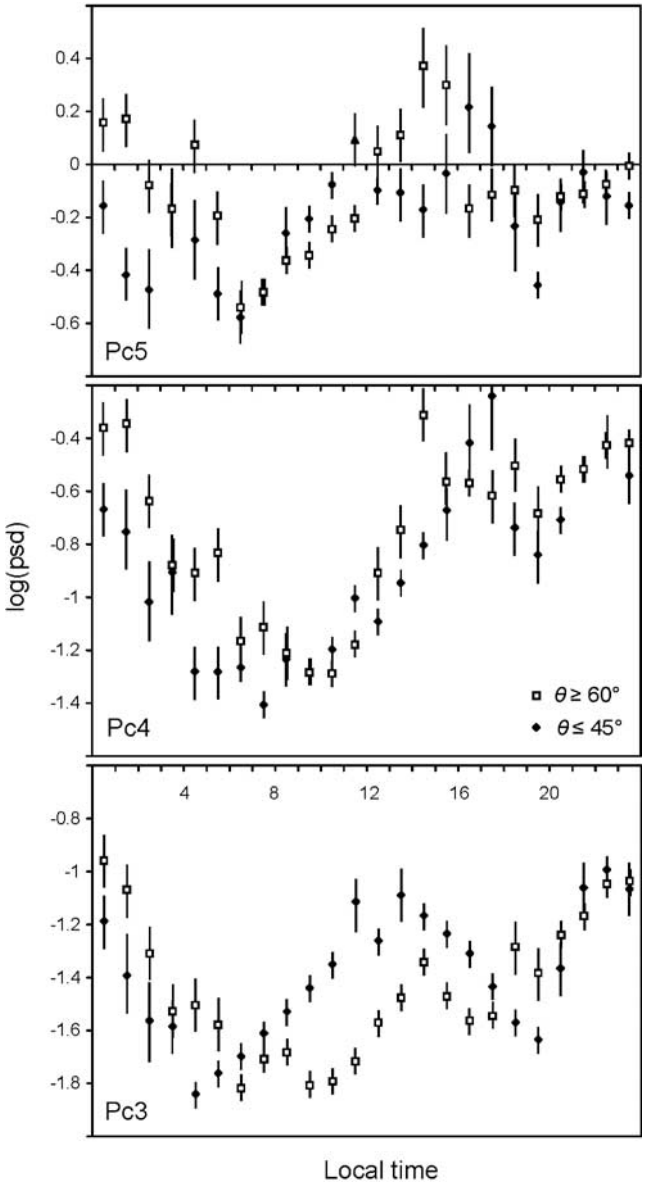

Figure 6. Global profiles of ULF wave power for IMF cone angle $\theta \geq 60°$ and $\theta \leq 45°$.

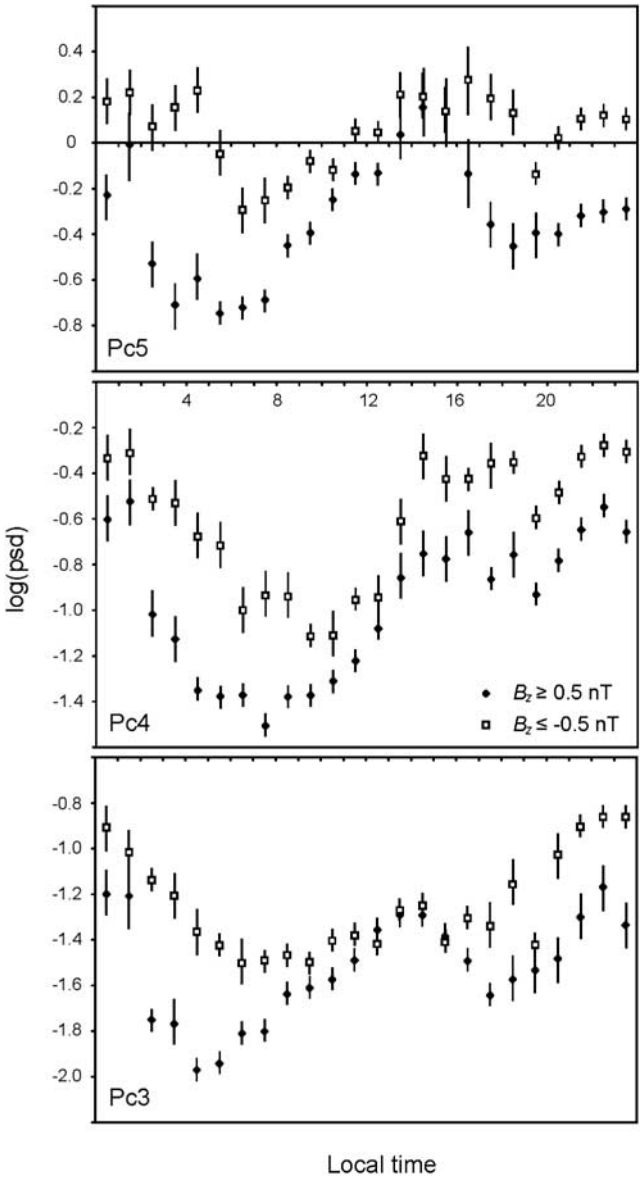

Figure 7. Global profiles of ULF wave power for northward and southward IMF.

comparison of dayside Pc5 wave power detected at ground stations to satellite observations of solar wind parameters by *Vennerstrøm* [1999] yielded a very weak correlation between power levels and IMF B_z.

[29] In our analysis of the local-time distribution of ULF wave power based on the north/south component of the IMF, we compared power observations for $B_z \geq 0.5$ nT and $B_z \leq -0.5$ nT, as shown in Figure 7. While there is some enhancement in the power for southward IMF, the increase is generally not as large as the increase observed for high solar wind velocity or pressure (Figures 3 and 4). ULF power, particularly in the Pc3 and Pc5 bands, appears to peak near local noon for northward IMF. As a result, the enhancement of wave power associated with IMF B_z is smaller on the dayside and larger on the nightside, in contrast to the power enhancement associated with solar wind velocity and pressure. Previous studies [*Francia et al.*, 1999; *Sanny et al.*, 2002] have found the response of the low-latitude geomagnetic field to be greater and correspond more closely to variations in the solar wind dynamic pressure during periods of northward IMF. This may account for the peak in the ULF power observed near local noon under this condition.

4. Summary and Future Work

[30] In this paper, we investigated the global local-time profiles of wave power in three ULF frequency bands corresponding to Pc3, Pc4, and Pc5 pulsations using magnetic field data from the geosynchronous GOES satellites. Power profiles were obtained for different levels of geomagnetic activity, season, and solar wind and IMF parameters.

[31] For high levels of geomagnetic activity, the greatest wave power was associated with compressional Pc5 pulsations in the afternoon and dusk sector. Smaller peaks in the morning sector in the Pc5 band and in the afternoon sector in the Pc4 band were also observed, while no peaks in the Pc3 wave power were found for high levels of geomagnetic activity. For low geomagnetic activity, the peak in the Pc5 power shifted to the prenoon sector and is probably due to pressure pulses. Other observations included a broad, low dayside peak in the Pc3 power, and elevated power levels for all three bands in the tail region, perhaps because of the occurrence of ULF waves during the quiet periods following high geomagnetic activity.

[32] Our study of the seasonal versus diurnal variation in the ULF power showed the presence of a summer minimum for all three frequency bands. The corresponding diurnal minima of the Pc5 and Pc3 bands were widely distributed on the dayside, while the Pc4 power minimum was localized around noon. Near the equinoxes, the power maxima for all three frequency bands were in the afternoon sector. Finally for all three bands, higher power levels were sustained around local midnight throughout the year, likely because of Pi activity associated with substorms.

[33] Both the solar wind velocity and the variability in the solar wind dynamic pressure exhibited strong influences on the ULF power levels. The greatest enhancement in the wave power due to higher solar wind velocities occurred over the entire dayside, while the power enhancement associated with increased pressure variability was global, with the greatest increase occurred for the lowest frequency waves. This latter result is consistent with previous work indicating that ULF pulsations in the magnetosphere are directly driven by variations in the solar wind dynamic pressure.

[34] The influence of the IMF on ULF wave power was studied using the cone angle and northward/southward orientation. The cone angle did not have any distinct effect on ULF wave power in the Pc5 and Pc4 bands. The only clear power enhancement occurred for the Pc3 band from about 9 LT to 13 LT for small values of the cone angle, providing further evidence that the upstream foreshock is the energy source of Pc3 pulsations.

[35] The dependence of ULF power on IMF B_z was not as pronounced as its dependence on solar wind velocity or dynamic pressure. Some power enhancement occurred for southward IMF, but on the nightside. ULF power, particu-

larly in the Pc3 and Pc5 bands, exhibited a prominent peak near local noon for northward IMF, perhaps because the response of the low-latitude geomagnetic field is greater and corresponds more closely to variations in the solar wind dynamic pressure during periods of northward IMF.

[36] The approach and database used in this project provide the framework for a future study involving the enhancement of relativistic electron fluxes during magnetic storms. We will develop a statistical "fingerprint" for moderate and intense magnetic storms based on time profiles of ULF power in the Pc3–Pc5 frequency bands as well as ULF power indices. By comparing this fingerprint to the pattern of relativistic electron flux, we hope to address some of the issues that have been raised in this area of study. These include (1) the differentiation between magnetic storms with relativistic electrons and magnetic storms without relativistic electrons, (2) the importance of broadband versus narrowband waves in the energization of relativistic electrons, and (3) the duration and timing of ULF power necessary to produce relativistic electrons.

[37] **Acknowledgments.** GOES data files used in this study were obtained from http://sd-www.jhuapl.edu, the Web site of the Johns Hopkins University Applied Physics Laboratory. Hourly values of the *Dst* index were obtained from the Web site of the World Data Center for Geomagnetism in Kyoto (http://swdcdb.kugi.kyoto-u.ac.jp). Hourly averages of solar wind and IMF parameters were downloaded from the OMNIWeb site of the National Space Science Data Center (http://nssdc.gsfc.nasa.gov/omniweb). Research at LMU was supported by NSF grant ATM-0350502. Research at IGPP/UCLA was supported by NSF grant ATM-0348398. Research at NASA/Goddard was supported by NASA's Guest Investigator Program.

[38] Zuyin Pu thanks Peter Chi and another reviewer for their assistance in evaluating this paper.

References

Anderson, B. J. (1994), An overview of spacecraft observations of 10 s to 600 s period magnetic pulsations in the Earth's magnetosphere, in *Solar Wind Sources of Magnetospheric Ultra-Low-Frequency Waves*, *Geophys. Monogr. Ser.*, vol. 81, edited by M. J. Engebretson, K. Takahashi, and M. Scholer, p. 25, AGU, Washington, D. C.

Anderson, B. J., M. J. Engebretson, S. P. Rounds, L. J. Zanetti, and T. A. Potemra (1990), A statistical study of Pc3–5 pulsations observed by the AMPTE/CCE magnetic fields experiment, 1. Occurrence distributions, *J. Geophys. Res.*, *95*, 10,495.

Arthur, C. W., and R. L. McPherron (1981), The statistical character of Pc4 magnetic pulsations at synchronous orbit, *J. Geophys. Res.*, *86*, 1325.

Baker, G. J., E. F. Donovan, and B. J. Jackel (2003), A comprehensive survey of auroral latitude Pc5 pulsation characteristics, *J. Geophys. Res.*, *108*(A10), 1384, doi:10.1029/2002JA009801.

Barfield, J. N., and R. L. McPherron (1978), Stormtime Pc5 magnetic pulsations observed at synchronous orbit and their correlation with the partial ring current, *J. Geophys. Res.*, *83*, 739.

Bevington, P. R., and D. K. Robinson (1992), *Data Reduction and Error Analysis for the Physical Sciences*, pp. 41–43, McGraw-Hill, New York.

Borovsky, J. E., and R. J. Nemzek (1994), Substorm statistics: occurrences and amplitudes, Tech. Rep. LA-UR-94-1378, Los Alamos National Laboratory, N. M.

Chi, P. J., C. T. Russell, and G. Le (1994), Pc 3 and Pc 4 activity during a long period of low interplanetary magnetic field cone angle as detected across the Institute of Geological Sciences array, *J. Geophys. Res.*, *99*(A6), 11,127.

Chi, P. J., C. T. Russell, R. M. Bloom, and H. J. Singer (1998), Solar wind control of ultralow-frequency wave activity at $L = 3$, *J. Geophys. Res.*, *103*(A12), 29,467.

Cliver, E. W., Y. Kamide, and A. G. Ling (2000), Mountains versus valleys: Semiannual variation of geomagnetic activity, *J. Geophys. Res.*, *105*(A2), 2413.

Dyrud, L. P., M. J. Engebretson, J. L. Posch, W. J. Hughes, H. Fukunishi, R. L. Arnoldy, P. T. Newell, and R. B. Horne (1997), Ground observations and possible source regions of two types of Pc 1–2 micropulsations at very high latitudes, *J. Geophys. Res.*, *102*(A12), 27,011.

Engebretson, M., K.-H. Glassmeier, M. Stellmacher, W. J. Hughes, and H. Lühr (1998), The dependence of high-latitude Pc5 wave power on solar wind velocity and on the phase of high-speed solar wind streams, *J. Geophys. Res.*, *103*(A11), 26,271.

Francia, P., S. Lepidi, U. Villante, P. Di Giuseppe, and A. J. Lazarus (1999), Geomagnetic response at low latitudes to continuous solar wind pressure variations during northward interplanetary magnetic field, *J. Geophys. Res.*, *104*, 19,923.

Greenstadt, E. W., J. V. Olson, P. D. Loewen, H. J. Singer, and C. T. Russell (1979a), Correlation of PC3, 4 and 5 activity with solar wind speed, *J. Geophys. Res.*, *84*, 6694.

Greenstadt, E. W., H. J. Singer, C. T. Russell, and J. V. Olson (1979b), IMF orientation, solar wind velocity, and Pc3-4 signals: A joint distribution, *J. Geophys. Res.*, *84*, 527.

Grubb, R. N. (1975), The SMS/GOES space environment monitor subsystem, NOAA Tech Memo, TM ERL SEL-42.

Howard, T. A., and F. W. Menk (2005), Ground observations of high-latitude Pc3-4 ULF waves, *J. Geophys. Res.*, *110*, A04205, doi:10.1029/2004JA010417.

Jacobs, J. A., Y. Kato, S. Matsushita, and W. A. Troitskaya (1964), Classification of geomagnetic micropulsations, *J. Geophys. Res.*, *69*, 180.

Junginger, H., and W. Baumjohann (1988), Dayside long period magnetospheric pulsations: Solar wind dependence, *J. Geophys. Res.*, *93*, 877.

Kepko, L., and H. E. Spence (2003), Observations of discrete, global magnetospheric oscillations directly driven by solar wind density variations, *J. Geophys. Res.*, *108*(A6), 1257, doi:10.1029/2002JA009676.

Kepko, L., H. E. Spence, and H. J. Singer (2002), ULF waves in the solar wind as direct drivers of magnetospheric pulsations, *Geophys. Res. Lett.*, *29*(8), 1197, doi:10.1029/2001GL014405.

Kokubun, S. (1985), Statistical character of Pc5 waves at geostationary orbit, *J. Geomagn. Geoelectr.*, *37*, 759.

Kokubun, S., K. N. Erickson, T. A. Fritz, and R. L. McPherron (1989), Local time asymmetry of Pc 4-5 pulsations and associated particle modulations at synchronous orbit, *J. Geophys. Res.*, *94*, 6607.

Lessard, M. R., M. K. Hudson, and H. Lühr (1999), A statistical study of Pc3–Pc5 magnetic pulsations observed by the AMPTE/Ion Release Module satellite, *J. Geophys. Res.*, *104*(A3), 4523.

Odera, T. J. (1986), Solar wind controlled pulsations: A review, *Rev. Geophys.*, *24*, 55.

Russell, C. T., and R. L. McPherron (1973), Semiannual variation of geomagnetic activity, *J. Geophys. Res.*, *78*, 92.

Sanny, J., J. A. Tapia, D. G. Sibeck, and M. B. Moldwin (2002), Quiet-time variability of the geosynchronous magnetic field and its response to the solar wind, *J. Geophys. Res.*, *107*(A12), 1443, doi:10.1029/2002JA009448.

Saito, H., N. Sato, Y. Tonegawa, T. Yoshino, and T. Saemundsson (1989), Seasonal and diurnal dependence of Pc 3-5 magnetic pulsation power at geomagnetically conjugate stations in the auroral zones, *J. Geophys. Res.*, *94*, 6945.

Sigsbee, K., C. A. Cattell, D. Fairfield, K. Tsuruda, and S. Kokubun (2002), Geotail observations of low-frequency waves and high-speed earthward flows during substorm onsets in the near magnetotail from 10 to 13 R_E, *J. Geophys. Res.*, *107*(A7), 1141, doi:10.1029/2001JA000166.

Southwood, D. J. (1979), Magnetopause Kelvin-Helmholtz instability, *Eur. Space Agency Spec. Publ.*, *SP-148*, 357.

Takahashi, K., and R. L. McPherron (1984), Standing hydromagnetic waves in the magnetosphere, *Planet. Space Sci.*, *32*, 1343.

Takahashi, K., and B. J. Anderson (1992), Distribution of ULF energy ($f <$ 80 mHz) in the inner magnetosphere: A statistical analysis of AMPTE CCE magnetic field data, *J. Geophys. Res.*, *97*(A7), 10,751.

Vennerstrøm, S. (1999), Dayside magnetic ULF power at high latitudes: A possible long-term proxy for the solar wind velocity?, *J. Geophys. Res.*, *104*(A5), 10,145.

Yumoto, K. A., A. Wolfe, T. Terasawa, E. L. Kamen, and L. J. Lanzerotti (1987), Dependence of Pc 3 magnetic energy spectra at southpole on upstream solar wind parameters, *J. Geophys. Res.*, *92*, 12,437.

Zhu, X., and M. G. Kivelson (1991), Compressional ULF waves in the outer magnetosphere 1. Statistical study, *J. Geophys. Res.*, *96*(A11), 19,451.

D. Berube and M. B. Moldwin, Institute of Geophysics and Planetary Physics, University of California, Los Angeles, CA, USA.

D. Judnick and J. Sanny, Physics Department, Loyola Marymount University, Los Angeles, CA, USA. (jsanny@lmu.edu)

D. G. Sibeck, NASA Goddard Space Flight Center, Greenbelt, MD, USA.